WARSAW UNIVERSITY OF TECHNOLOGY Index 351733
FACULTY OF CIVIL ENGINEERING
COMMITTEE FOR CIVIL AND WATER ENGINEERING
POLISH ACADEMY OF SCIENCES ISSN 1230-2945
DOI: 10.24425/ace.2026.158612
ARCHIVES OF CIVIL ENGINEERING
Vol. LXXII ISSUE 2 2026
pp. 331 –345

Research paper

Calculation method of stress and deformation of hinged frame beams based on Winkler model

Benqian Wang[1], Shibin Kang[2], Peng Tan[3], Guozeng Liu[4]

Abstract: Abstract: Based on Winkler foundation model, the mechanical model and coordinate system of hinged prefabricated anchor frame beam were established in order to quantitatively study the mechanical deformation characteristics of hinged prefabricated anchor beam. The mechanical model of hinged frame beams is simplified to Winkler elastic foundation beams. First, the general solution of beam bottom displacement is obtained by establishing the differential equation of beam deflection line, and then the general solution for rotation angle, bending moment and shearing force of the beam is obtained according to the relationship among beam bottom displacement, rotation angle, bending moment and shear force. The motion equation for the beam is derived based on the boundary and continuity conditions of the hinged frame beam. Then, the difference of structural characteristics between hinged frame beams and traditional frame beams under different anchoring forces is compared. Finally, the influence of external factors (anchorage force, foundation reaction coefficient) and internal factors (section size, cantilever length, hinged position) on the stress and deformation characteristics of the frame beam is compared, and the influence law of various factors is obtained by comparison, which provides a reference for the standardized design of the hinged frame beam.

Keywords: deformation characteristic, dynamic calculation model, hinged prefabricated anchor frame beam, numerical simulation, slope engineering

[1]Eng., China Road and Bridge Corporation, 100011, Beijing, China, e-mail: lgz0310@163.com, ORCID: 0009-0003-6173-5780
[2]Eng., China Road and Bridge Corporation, 100011, Beijing, China, e-mail: 1440906523@qq.com, ORCID: 0009-0006-2816-0227
[3]Eng., China Road and Bridge Corporation, 100011, Beijing, China, e-mail: 3984915311@qq.com, ORCID: 0009-0002-6466-4079
[4]MSc., School of Traffic and Transportation Engineering, Changsha University of Science & Technology, Changsha 410114, China, e-mail: l17838553713@.126.com, ORCID: 0009-0005-3158-2554

1. Introduction

In recent years, with the rapid development of infrastructure such as highways and railways, there has been an increasing emphasis on landslide management in engineering, leading to the emergence of various forms of retaining walls, anti-slip piles, anchor rods, and anchor cables as support structures [1–5]. Due to its relatively mature technology, frame beams are widely used in slope support engineering. In order to make the force of the frame beam more reasonable and stable, the researchers have proposed combining the anchor and the frame beam. However this construction method still presents numerous issues within frame beam technology, such as poor support timeliness, difficulties in deformation coordination, high construction requirements, and significant construction risks, which makes the frame beam still has many problems in the application [6]. An hinged prefabricated anchor frame beam structure is proposed in "Guide to Slope Anchoring with Articulated Assembled Frame Beams" [7]. In this structure, the frame beams are composed of three parts, namely prefabricated transverse and longitudinal beams and prefabricated cross beams, and the longitudinal beams are articulated with the cross beams. Compared with the traditional frame beams, the hinged frame beams are able to better adapt to the deformation of the slopes, which has been demonstrated the rationality of the hinged frame beams by comparative studies [8–11].

In the calculation of internal force and deformation of anchor beam frame, the researchers carried out research by Winkler elastic foundation model, two-parameter model, three-parameter model and semi-infinite body foundation model, including [12–15]. Various beam theories have been applied, such as Bernoulli-Euler and Timoshenko theory, etc. Many researchers have discussed the analytical solution of internal forces of frame beams under the Bernoulli-Euler and Timoshenko beam theories, including [16], but they lack the analytical calculation of hinged beams. In the analysis of internal forces and deformation of beams, analytical method and finite element method are widely used, including [17]. This paper also solves the internal forces and deformation of frame beams by analytical method. Zhu et al. [18] formulated the traditional frame beam as a finite transverse and longitudinal beam closely adhering to the slope surface, based on the elastic assumption of the traditional frame beam and the deformation coordination condition of the elastic foundation model, and solved to obtain the analytical solutions of the deformation, bending moment and shear force of the traditional frame beam, which revealed the interaction mechanism of the traditional frame beam and the rock body of the slope. Han et al. [19] calculated the internal forces of conventional frame beam system by inverted beam method, illustrating the internal force distribution of beams under pre-stressing stage and limit state stage of conventional frame beams.

Based on the theory of Winkler elastic foundation beams, this paper obtains the special solutions for the displacement, angle, beam moment and shear force of the beams by establishing the differential equations for the beam deflection curves and combining them with the boundary conditions in the practical application of hinged frame beams as well as the continuity conditions at the hinged points. Afterwards, the above equations show the differences in the force and deformation characteristics between hinged frame beams and traditional cast-in-place frame beams; the influence of anchorage force and foundation reaction coefficient on the force characteristics of hinged frame beams; and the influence of cross-section dimensions, cantilever lengths and hinged positions on hinged frame beams.

2. Calculation of internal force and deformation of articulated assembled anchor frame beams

As shown in Fig. 1, the hinged anchor frame beam composed of simplified three-section prefabricated beam structure is used as a representative, which serves as a unit in the hinged frame beam system. This system consists of three prefabricated beams that can rotate vertically at the connection points, viewed as hinge points. At these points, deflection and shear force are continuous, while the bending moment is zero. The foundation action is simplified to spring action, and the mechanical model is established as shown in Fig. 2. Taking the left endpoint of the hinged anchor frame beam as the origin and the beam's length direction as the axis direction, a coordinate system is established. The coordinates of points A, B, C, D, E, and F from left to right are (0,0), (L_1,0), (l_1,0), (l_2,0), (L_3,0), and (l_3,0), respectively. P_1 represents the concentrated force on the first beam segment, acting at point B; P_3 represents the concentrated force on the third beam segment, acting at point E.

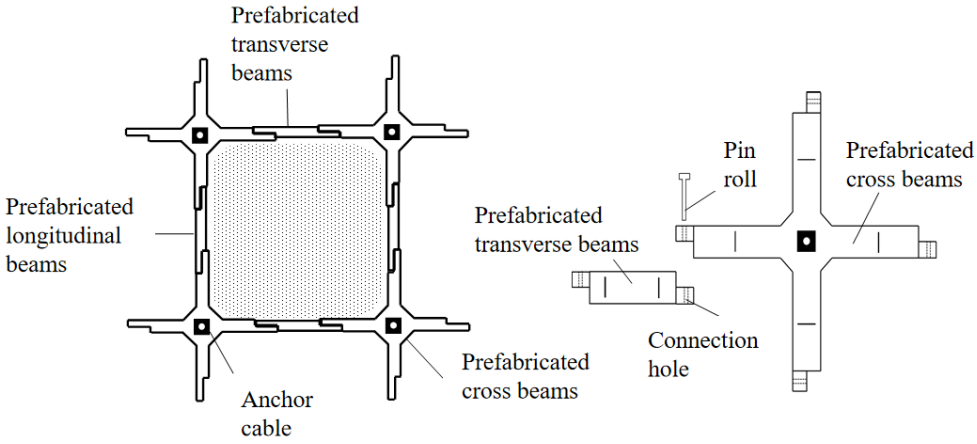

Fig. 1. Hinged type assembled beam frame structure schematic [10]

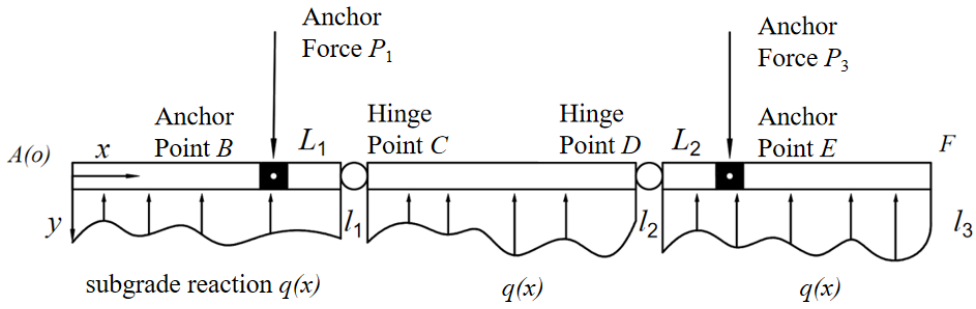

Fig. 2. Mechanical model and coordinate system of articulated assembled bolt frame beam

Based on the Winkler foundation model, the force P at any point on the surface of the beam is proportional to the displacement at that point with the following equation:

$$P(x) = kw\,(x) \tag{2.1}$$

where: k – foundation reaction factor, $w(x)$ – vertical displacement at any point on the surface of the hinged anchor frame beam.

The differential equation for the deflection curve of the beam is obtained from Eq. (2.1) as:

$$EI\frac{d^4w(x)}{\mathrm{d}x^4} = -bkw\,(x) \tag{2.2}$$

where: E – modulus of elasticity of hinged prefabricated anchor frame beam, I – moment of inertia in the cross-section of articulated assembled anchor frame beams $I = \dfrac{bh^3}{12}$, h – height of articulated assembled anchor frame beams, b – width of articulated assembled anchor frame beams.

Let $w(x) = e^{\lambda x}$, λ is a defined intermediate variable $\lambda = \sqrt[4]{\dfrac{kb}{4EI}}$, substituting this into Eq. (2.2) yields a generalized solution for the vertical displacement of the articulated beam as:

$$w(x) = e^{\lambda x}(C_1\cos\lambda x + C_2\sin\lambda x) + e^{-\lambda x}(C_3\cos\lambda x + C_4\sin\lambda x) \tag{2.3}$$

where: C_1, C_2, C_3 and C_4 – the constant of integration, determined from the boundary conditions of the articulated frame beam.

Afterwards, the expressions for the angle, bending moment, and shear force can be determined from the relationship between the displacement at the bottom of the beam and the angle, bending moment, and shear force.

The role of anchoring force needs to be considered in this model, where $x \geq x_P$ (location of anchoring force), the displacement under anchoring force can be obtained from Eq. (2.3):

$$w(x_P) = \frac{P}{4\lambda^3 EI}\left[ch(\lambda x)\sin(\lambda x) - sh(\lambda x)\cos(\lambda x)\right] \tag{2.4}$$

Associating Eq. (2.4) and the boundary condition and continuity condition of the frame beam yields the displacement generalization of the beam as:

$$\begin{aligned} w_i(x) = {} & e^{\lambda x}\left(C_{4i-3}\cos\lambda x + C_{4i-2}\sin\lambda x\right) + e^{-\lambda x}\left(C_{4i-1}\cos\lambda x + C_{4i}\sin\lambda x\right) \\ & + \sum_0^i \frac{P_i}{4\lambda^3 EI}\begin{bmatrix} ch\lambda\left(x - x_{P_i}\right)\sin\lambda\left(x - x_{P_i}\right) \\ -sh\lambda\left(x - x_{P_i}\right)\cos\lambda\left(x - x_{P_i}\right) \end{bmatrix} u\left(x - x_{P_i}\right) \end{aligned} \tag{2.5}$$

where: $C_{4i-3} \sim C_{4i}$ – undetermined constant of section i beam, i – the number of beams ($i = 1, 2, 3$), P_i – anchoring force, $u\left(x - x_{P_i}\right)$ – the Heaviside function.

$$u\left(x - x_{P_i}\right) = \begin{cases} 0 & 0 \leq x < x_{P_i} \\ 1 & x \geq x_{P_i} \end{cases}$$

$$P_i = \begin{cases} P_i & i = 1,3 \\ 0 & i = 2 \end{cases}$$

The angle θ, bending moment M, and shear force Q of the frame beam section are related to the displacement:

$$\left.\begin{aligned} \theta &= \frac{\mathrm{d}w}{\mathrm{d}x} \\ M &= -EI\frac{\mathrm{d}^2w}{\mathrm{d}x^2} \\ Q &= -EI\frac{\mathrm{d}^3w}{\mathrm{d}x^3} \end{aligned}\right\} \tag{2.6}$$

The couplings (2.5) and (2.6) can obtain the generalized solution of beam angle θ, bending moment M, and shear force Q:

$$\begin{aligned} \theta_i(x) = {} & \lambda e^{\lambda x}(C_{4i-3}\cos\lambda x + C_{4i-2}\sin\lambda x - C_{4i-3}\sin\lambda x + C_{4i-2}\cos\lambda x) \\ & + \lambda e^{-\lambda x}(-C_{4i-1}\cos\lambda x - C_{4i}\sin\lambda x - C_{4i-1}\sin\lambda x + C_{4i}\cos\lambda x) \\ & + \sum_0^i \frac{P_i}{2\lambda^2 EI} sh\lambda\left(x - x_{P_i}\right)\sin\lambda\left(x - x_{P_i}\right)u\left(x - x_{P_i}\right) \end{aligned} \tag{2.7}$$

$$\begin{aligned} M_i(x) = {} & -2\lambda^2 EI\left[\begin{array}{l} e^{\lambda x}(-C_{4i-3}\sin\lambda x + C_{4i-2}\cos\lambda x) + \\ e^{-\lambda x}(C_{4i-1}\sin\lambda x - C_{4i}\cos\lambda x) \end{array}\right] \\ & - \sum_0^i \frac{P_i}{2\lambda}\left[\begin{array}{l} ch\lambda\left(x - x_{P_i}\right)\sin\lambda\left(x - x_{P_i}\right) + \\ sh\lambda\left(x - x_{P_i}\right)\cos\lambda\left(x - x_{P_i}\right) \end{array}\right] u\left(x - x_{P_i}\right) \end{aligned} \tag{2.8}$$

$$\begin{aligned} Q_i(x) = {} & -2\lambda^3 EI\left[\begin{array}{l} e^{\lambda x}(-C_{4i-3}\sin\lambda x + C_{4i-2}\cos\lambda x \\ -C_{4i-3}\cos\lambda x - C_{4i-2}\sin\lambda x) + \\ e^{-\lambda x}(-C_{4i-1}\sin\lambda x + C_{4i}\cos\lambda x \\ +C_{4i-1}\cos\lambda x + C_{4i}\sin\lambda x) \end{array}\right] \\ & - \sum_0^i P_i ch\lambda\left(x - x_{P_i}\right)\cos\lambda\left(x - x_{P_i}\right)u\left(x - x_{P_i}\right) \end{aligned} \tag{2.9}$$

where: $\theta_i(x)$ – angle of turn of the i beam under the action of the concentrated force P_i, $M_i(x)$ – the bending moment of section i of the beam under the action of the concentrated force P_i, $Q_i(x)$ – the shear force in section i of the beam under the action of the concentrated force P_i.

The constants of integration in the example can be obtained from the boundary conditions of the articulated frame beam [20].

For the first section of the beam:

The bending moment M_{1C} is zero at point C (segment AC) ($M_{1C} = 0$):

$$P_1\left(l_1 - L_1\right) - kb\int_0^{l_1}(l_1 - x)\left[\begin{array}{l} e^{\lambda x}(C_1\cos\lambda x + C_2\sin\lambda x) + \\ e^{-\lambda x}(C_3\cos\lambda x + C_4\sin\lambda x) \end{array}\right]\mathrm{d}x = 0 \tag{2.10}$$

The bending moment M_{1A} is zero at point A ($M_{1A} = 0$):

$$2\lambda^2 EI(-C_2 + C_4) = 0 \tag{2.11}$$

The shear force Q_{1A} is zero at point A ($Q_{1A} = 0$):

$$-EI\frac{\mathrm{d}^3 w_1(x)}{\mathrm{d}x^3}\bigg|_{x=0} = 2\lambda^3 EI\,(C_1 - C_2 - C_3 - C_4) = 0 \tag{2.12}$$

For the second section of the beam:
Shear continuity on both sides of point C ($Q_{1C} - Q_{2C} = 0$):

$$\begin{aligned}2\lambda^3 EI[e^{\lambda x}(&+C_1\sin\lambda x - C_2\cos\lambda x + C_1\cos\lambda x + C_2\sin\lambda x - C_5\sin\lambda x + \\ &C_6\cos\lambda x - C_5\cos\lambda x - C_6\sin\lambda x) + e^{-\lambda x}(+C_3\sin\lambda x - C_4\cos\lambda x - C_3\cos\lambda x - \\ &C_4\sin\lambda x - C_7\sin\lambda x + C_8\cos\lambda x + C_7\cos\lambda x + C_8\sin\lambda x)] = 0\end{aligned} \tag{2.13}$$

Shear continuity on both sides of point D ($Q_{2C} - Q_{3C} = 0$):

$$\begin{aligned}2\lambda^3 EI[e^{\lambda x}(&+C_5\sin\lambda x - C_6\cos\lambda x + C_5\cos\lambda x + C_6\sin\lambda x - C_9\sin\lambda x + \\ &C_{10}\cos\lambda x - C_9\cos\lambda x - C_{10}\sin\lambda x) + e^{-\lambda x}(+C_7\sin\lambda x - C_8\cos\lambda x - \\ &C_7\cos\lambda x - C_8\sin\lambda x - C_{11}\sin\lambda x + C_{12}\cos\lambda x + C_{11}\cos\lambda x + C_{12}\sin\lambda x)] = 0\end{aligned} \tag{2.14}$$

The displacements on either side of point C are equal ($W_{1C} = W_{2C}$):

$$\begin{aligned}&e^{\lambda l_1}(C_1\cos\lambda l_1 + C_2\sin\lambda l_1 - C_5\cos\lambda x l_1 - C_6\sin\lambda l_1) + \\ &e^{-\lambda l_1}(C_3\cos\lambda l_1 + C_4\sin\lambda l_1 - C_7\cos\lambda l_1 - C_8\sin\lambda l_1) = 0\end{aligned} \tag{2.15}$$

The displacements on either side of point D are equal ($W_{2D} = W_{3D}$):

$$\begin{aligned}&e^{\lambda l_2}\,(C_5\cos\lambda l_2 + C_6\sin\lambda l_2 - C_9\cos\lambda l_2 - C_{10}\sin\lambda l_2) + \\ &e^{-\lambda l_2}\,(C_7\cos\lambda l_2 + C_8\sin\lambda l_2 - C_{11}\cos\lambda l_2 - C_{12}\sin\lambda l_2) = 0\end{aligned} \tag{2.16}$$

The bending moment M_{2C} is zero at point C ($M_{2C} = 0$):

$$-2\lambda^2 EI\left[e^{\lambda l_1}(-C_5\sin\lambda l_1 + C_6\cos\lambda l_1) + \lambda^2 e^{-\lambda l_1}(C_7\sin\lambda l_1 - C_8\cos\lambda l_1)\right] = 0 \tag{2.17}$$

The bending moment M_{2D} at point D is zero the ($M_{2D} = 0$):

$$-2\lambda^2 EI\left[e^{\lambda l_2}(-C_5\sin\lambda l_2 + C_6\cos\lambda l_2) + e^{-\lambda l_2}(C_7\sin\lambda l_2 - C_8\cos\lambda l_2)\right] = 0 \tag{2.18}$$

For the third section of the beam:
Equilibrium of bending moments at point D (section DF) ($M_{3D} = 0$):

$$P_3\,(L_3 - l_2) - \int_{l_2 l_3}(x - l_2)kb\left[e^{\lambda x}\begin{pmatrix} C_9\cos\lambda x + \\ C_{10}\sin\lambda x\end{pmatrix} + e^{-\lambda x}\begin{pmatrix} C_{11}\cos\lambda x \\ +C_{12}\sin\lambda x\end{pmatrix}\right]\mathrm{d}x = 0 \tag{2.19}$$

The bending moment at point F is zero ($M_{3F} = 0$):

$$-2\lambda^2 EI\left[e^{\lambda l_3}(-C_9\sin\lambda l_3 + C_{10}\cos\lambda l_3) + \lambda^2 e^{-\lambda l_3}(C_{11}\sin\lambda l_3 - C_{12}\cos\lambda l_3)\right] = 0 \tag{2.20}$$

The shear force at point F is zero ($Q_{3F} = 0$):

$$\begin{aligned}-2\lambda^3 EI\left[e^{\lambda l_3}(-C_9\sin\lambda l_3 + C_{10}\cos\lambda l_3 - C_9\cos\lambda l_3 - C_{10}\sin\lambda l_3)\right.\\ \left. + e^{-\lambda l_3}(-C_{11}\sin\lambda l_3 + C_{12}\cos\lambda l_3 + C_{11}\cos\lambda l_3 + C_{12}\sin\lambda l_3)\right] = 0\end{aligned} \tag{2.21}$$

Associative Eq. (2.10)–(2.21), $C_1 - C_{12}$ can be obtained, and after that, substituting into Eq. (2.5) as well as (2.7)–(2.9), the definite expressions for the displacement, angle, bending moment, and shear force of the articulated beam can be obtained.

3. Case analysis

The constant expressions for the bottom displacement, corner, bending moment and shear force of the hinged frame beam solved in the previous section can be used to analyze the factors affecting the force characteristics of this beam. The values of each of these parameters are given in Table 1. The assigned anchorage force P reference in the Table 1 is taken as 345 kN [10].

Table 1. Calculating parameters for model

Length of single section L [m]	**Anchor spacing Y [m]**	**Frame beam width b [m]**	**Frame beam height h [m]**
2	3×3	0.3	0.4
Foundation reaction factor k [kN/m^3]	**Anchor force P [kN]**	**Modulus of elasticity of concrete E [GPa]**	**Articulation point – anchor point distance L [m]**
4×104	345	30	0.5

3.1. Verification and comparison of equation solutions

In order to verify the rationality of the calculation method deduced in this paper, the structural model of this paper is degraded to a single beam subjected to concentrated force and the corresponding solution in the literature [21] is compared and analyzed. For facilitating its comparison, $L_1 = 5$ m, $l_1 = 10$ m, the concentrated force is taken as $P = 400$ kN and $0.5P = 200$ kN, respectively, while the other parameters are kept in the same way as those in the literature [22]. From the comparison of the two in Fig. 3, it can be seen that the force deformation curves of the beam are in perfect agreement, so the rationality of the special solution expression in this paper can be verified.

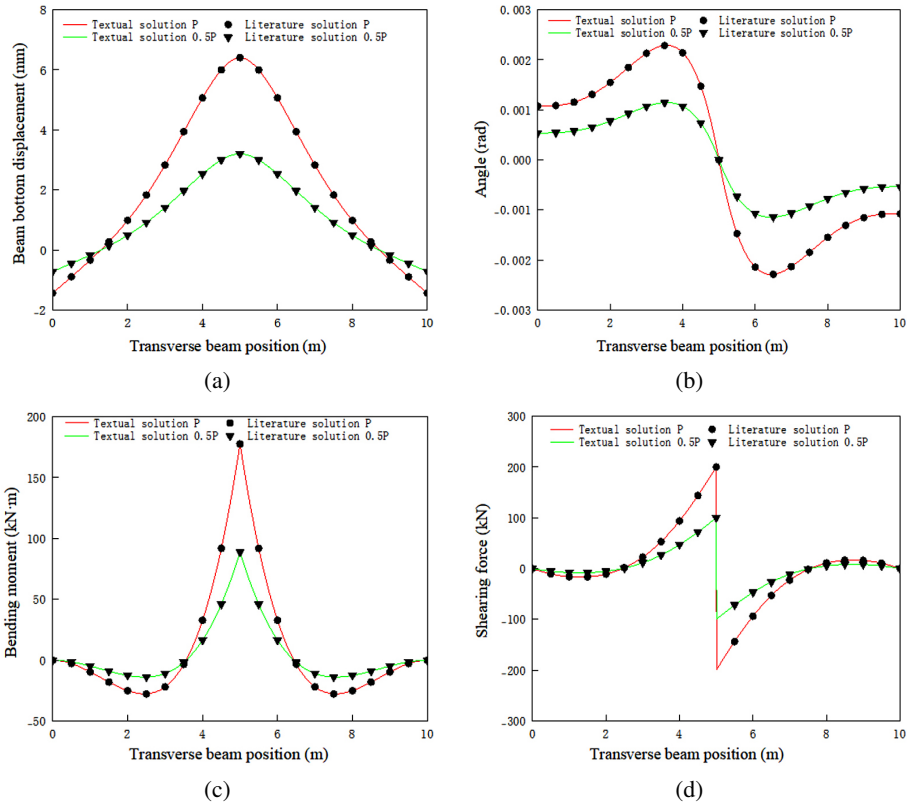

Fig. 3. Displacement, rotation Angle, Bending moment and Shear force diagram of the beam solved in this paper and in the literature: (a) Transverse beam displacement, (b) Transverse beam angle, (c) Transverse beam bending moment, (d) Transverse beam shear force

3.2. Comparison of force and deformation characteristics of articulated frame beams and conventional framebeams

In order to compare the force and deformation characteristics between traditional frame beams and hinged prefabricated anchor frame beam, the change curves of the bottom displacement, corner, bending moment and shear force of both traditional frame beams and hinged prefabricated anchor frame beam about the position of the beams are shown in Fig. 4 with different concentration forces ($0.8P$, $1.5P$), which are calculated using the method for the traditional frame beams proposed in literature [23], and calculated using the method mentioned above for articulated assembled anchor frame beams. From the observation of Fig. 4, it can be seen that the trends of the bottom beam displacements, angles, bending moments, and shear forces of the two beam structures are similar in general under the conditions of changes in the position of the crossbeam. In Fig. 4(c) and (d), the bending moment and shear force of the articulated beams on both sides of the beams are smaller than those of the conventional

cast-in-place beams; in the middle part of the beams, the bending moment of the articulated beams is smaller than those of the conventional cast-in-place beams, with an average bending moment of about 75% of that of the conventional cast-in-place beams, and the average shear force of the articulated beams is about 7% higher than that of the conventional cast-in- place beams. The overall analysis shows that the design of the articulated beam effectively reduces the bending moment of the beam structure.

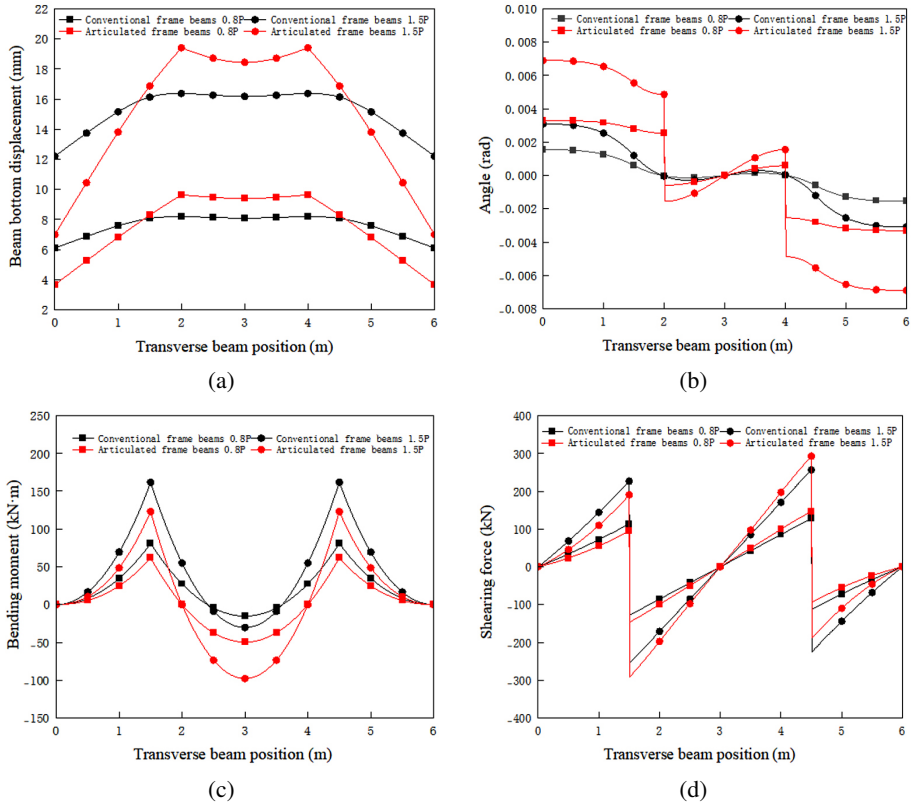

Fig. 4. Comparison of displacement, Angle, Bending moment and Shear force between articulated type and traditional frame beam: (a) Transverse beam displacement, (b) Transverse beam angle, (c) Transverse beam bending moment, (d) Transverse beam shear force

3.3. Parametric analysis of force deformation in articulated frame beam structures

To further investigate the structural force characteristics of the articulated beam structure. Figure 5 shows the variation of the bottom displacement, beam turning angle, bending moment, and shear force of the articulated assembled frame beams with the position of the crossbeam

under the action of different concentrated forces (0.6P, 0.8P, 1.0P, and 1.2P), respectively. In Fig. 5(c), the bending moment of the beam structure is 0 kN·m at 0 m, 2 m, 4 m and 6 m of the beam position under different concentrated forces, which is manifested by the boundary condition that the bending moment is 0 kN·m at both sides of the free ends of the articulated beam structure and at the articulation point, and the points of great value of the bending moment correspond to 1.5 m, 3 m and 4.5 m of the beam position. In Fig. 5(d), the articulated beams under different concentrated forces have a shear force of 0kN at the two end points (0 m, 6 m), which is shown as the boundary condition of shear force at the free end of the beams. A sudden change occurs at the beam position of 1.5 m, 4.5 m and the value of the sudden change is the magnitude of the concentrated force at the point; and the shear force is continuous at the beam position of 2 m, 4 m. By changing the magnitude of the concentrated force in the articulated assembled anchor frame beam, the reasonableness of the model derived from this paper can be observed from the Fig. 5.

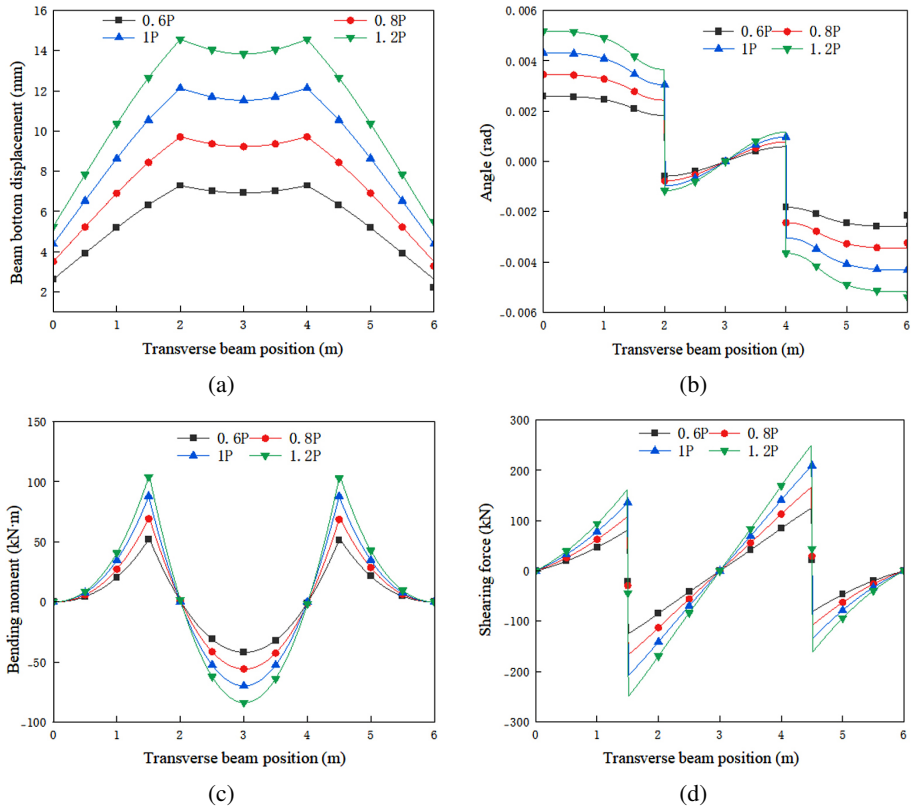

Fig. 5. Displacement, Angle, Bending moment and Shear of articulated frame beams under different anchoring forces: (a) Transverse beam displacement, (b) Transverse beam angle, (c) Transverse beam bending moment, (d) Transverse beam shear force

Figure 6 compares the changes of the bottom displacement, beam angle, bending moment and shear force of the articulated assembled anchor frame beam girder with respect to the position of the crossbeam under the action of different foundation reaction coefficients, where the values of the foundation reaction coefficients are taken as $K_1 = 1.5 \times 10^5$ kN/m^3, $K_2 = 3 \times 10^5$ kN/mm^3, $K_3 = 4.5 \times 10^5$ kN/m^3, $K_4 = 6 \times 10^5$ kN/mm^3, $K_5 = 7.5 \times 10^5$ kN/m^3. In Fig. 6(a) and (b), it can be clearly observed that with the increase of foundation reaction force coefficient, the beam bottom displacement and beam turning angle significantly decrease, which is in line with the characteristics of Winkler foundation model [24]. In Fig. 6(c) and (d), the change of foundation reaction force coefficient has little effect on the bending moment and shear force on the beam.

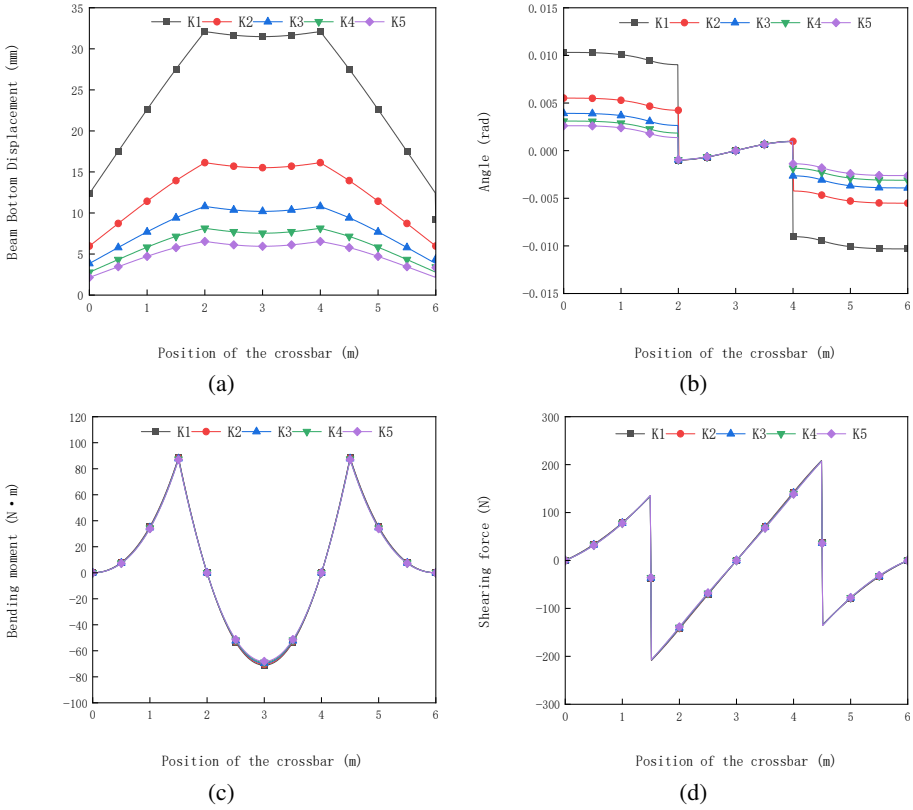

Fig. 6. Displacement, rotation Angle, Bending moment and Shear force of frame beams under different foundation reaction coefficients: (a) Transverse beam displacement, (b) Transverse beam angle, (c) Transverse beam bending moment, (d) Transverse beam shear force

Figure 7 compares the variation of beam bottom displacement, beam turning angle, bending moment, and shear force of articulated assembled anchor frame beams with respect to the position of the crossbeam under different conditions of cross-section dimensions, which are taken as $S_1 = 0.15 \times 0.25$ m, $S_2 = 0.3 \times 0.4$ m, $S_3 = 0.45 \times 0.55$ m, $S_4 = 0.6 \times 0.7$ m. In

Fig. 7(a) and (b), the beam bottom displacement and beam turning angle decrease with the increase of section size, which is manifested by the decrease of beam deformation when the beam is subjected to external force, but the decrease is smaller with the increase of section size. In Fig. 7(c) and (d), the bending moment and shear force are minimally affected by the change in cross-section size. In summary, the change of section size mainly affects the degree of force deformation of the beam. When selecting the cross-section size, combined with the economy can appropriately increase the cross-section size to reduce the force deformation of the articulated type assembled anchor frame beam.

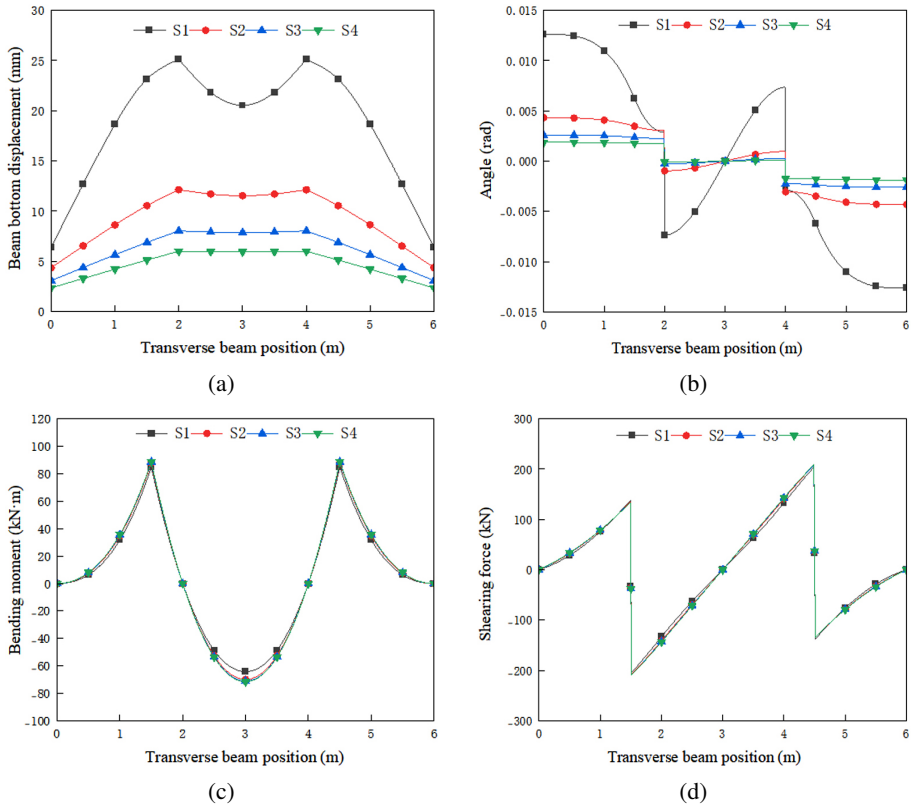

Fig. 7. Displacement, rotation Angle, Bending moment and Shear force diagram of frame beam under different section sizes: (a) Transverse beam displacement, (b) Transverse beam angle, (c) Transverse beam bending moment, (d) Transverse beam shear force

Figure 8 shows the variation of beam bottom displacement, beam turning angle, bending moment, and shear force of articulated assembled anchor frame beams with respect to the position of the beams under different cantilever lengths, where the cantilever lengths are X_1 = 0.5 m, X_2 = 0.75 m, X_3 = 1.0 m, X_4 = 1.25 m, and X_5 = 1.5 m, and the cantilever lengths are the lengths of the beams from the free end to the anchorage points. In Fig. 8(c)

and (d), the maximum values of bending moments at anchorage points and mid-span both decrease significantly with decreasing cantilever length, while the shear force also decreases with decreasing cantilever length at anchorage points. In summary, in the fabrication of articulated assembled anchor frame beams, the force condition and performance of the beam structure can be improved by reasonably shortening the cantilever length.

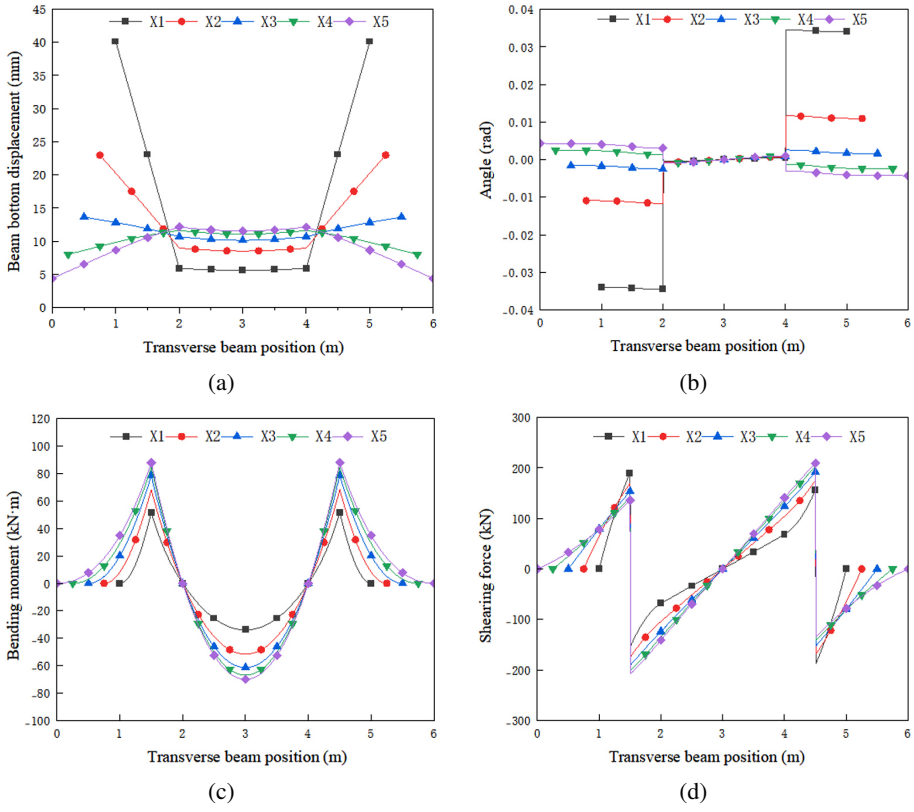

Fig. 8. Displacement, Angle, Bending moment and Shear of frame beam under different cantilever lengths: (a) Transverse beam displacement, (b) Transverse beam angle, (c) Transverse beam bending moment, (d) Transverse beam shear force

4. Conclusions

In this paper, based on Winkler elastic foundation beam theory, the mechanical model and coordinate system of articulated assembled anchor frame beam structure are established. Based on the mechanical model and coordinate system, the general solutions of displacement, corner, bending moment, and shear force at the bottom of articulated frame beam under the action of centralized force are computed; and calculate its definite solution through its boundary condi-

tions and continuity conditions at the articulation. which can accurately determine the structural internal force of the beam for structural design. The following conclusions were mainly obtained:

1. Comparing the internal force and deformation of articulated frame beams and conventional frame beams, the articulated frame beams, due to the articulated structure, make the change of displacement and angle of the bottom of the beams larger than that of the conventional frame beams after the beams are subjected to soil pressure, and the maximum bending moment of the beams is reduced by about 25% compared with that of the conventional frame beams.
2. The internal force and deformation of articulated frame beam is positively correlated with the anchorage force; the foundation reaction force coefficient has negligible influence on the bending moment and shear force of the frame beam, and negatively correlates with the displacement and angle of the beam; the structure of the articulated frame beam itself can be selected through the coordination of the beam's deformation and the force, which makes the articulated frame beam have better structural characteristics.

Acknowledgements

This work is supported by one project: China Communications Construction Company Youth Innovation Project, the project number is 2021-ZJKJ-QNCX17.

References

[1] M. Yan, Y. Xia, T. Liu, and V.M. Bowa, "Limit analysis under seismic conditions of a slope reinforced with prestressed anchor cables", *Computers and Geotechnics*, vol. 108, pp. 226–233, 2019, doi: 10.1016/j.compgeo.2018.12.027.

[2] K. Shi, X. Wu, Z. Liu, and S. Dai, "Coupled calculation model for anchoring force loss in a slope reinforced by a frame beam and anchor cables", *Engineering Geology*, vol. 260, art. no. 105245, 2019, doi: 10.1016/j.enggeo.2019.105245.

[3] J. Wang and F. Ying, "Research on the design method of flexural capacity of RC beams strengthen by ultra-high-performance concrete", *Archives of Civil Engineering*, vol. 70, no. 1, pp. 487–507, 2024, doi: 10.24425/ace.2024.148924.

[4] J. Feng, J. Chen, J. Li, Y. Zhang, J. Guo, and H. Qiu, "An early warning method for a slope based on the increment ratio of anchor cable internal force", *Archives of Civil Engineering*, vol. 69, no. 1, pp. 553–569, 2023, doi: 10.24425/ace.2023.144188.

[5] L.B. Abdalla, K. Ghafor, and A. Mohammed, "Testing and modeling the young age compressive strength for high workability concrete modified with PCE polymers", *Results in Materials*, vol. 1, art. no. 100004, 2019, doi: 10.1016/j.rinma.2019.100004.

[6] M. Zawam, K. Soudki, and J.S. West, "Factors affecting the time-dependent behaviour of GFRP prestressed concrete beams", *Journal of Building Engineering*, vol. 24, art. no. 100715, 2019, doi: 10.1016/j.jobe.2019.02.007.

[7] J. Zhang, F. Li, and S. Zhang, "Technical Guidelines for Slope Anchoring of Articulated Assembly Frame Beams", Changsha University of Science and Technology, China, 2024.

[8] J. Zhang, Q. Zhou, and L. Feng, "A Review of the progress of research on slope support structures anchored by frame beams", *Journal of China & Foreign Highway*, vol. 43 no. 03, pp. 17–23, 2023, doi: 10.14048/j.issn.1671-2579.2023.03.002.

[9] X. Sun, L. Wang, and R. Yu, "Experimental study on degradation of flexural performance of corroded stainless steel bars reinforced concrete beam", *Journal of Building Structures*, vol. 42, no. 6, pp. 160–168, 2021, doi: 10.14006/j.jzjgxb.2019.0510.

[10] F. Li. "Study on the mechanism of slope support and seismic dynamic characteristics of articulated frame beam anchored slopes", Changsha University of Science and Technology, China, 2021.

[11] Y. Zhang, Y. Qin, and H. Wang. "Research on performance of prefabricated beam-column hinged frame-shear wall structure system", *Building Structure*, vol. 53, no. 19, pp. 71–75+67, 2023, doi: 10.19701/j.jzjg.SJD2306.

[12] J. Gao, W. Yao, and J. Liu, "Temperature stress analysis for bi-modulus beam placed on Winkler foundation", *Applied Mathematics and Mechanics*, vol. 38, no. 7, pp. 921–934, 2017, doi: 10.1007/s10483-017-2216-6.

[13] K. Morfidis and I.E. Avramidis, "Formulation of a generalized beam element on a two-parameter elastic foundation with semi-rigid connections and rigid offsets", *Computers & Structures*, vol. 80, no. 25, pp. 1919–1934, 2002, doi: 10.1016/S0045-7949(02)00226-2.

[14] N. Tullini and A. Tralli, "Static analysis of Timoshenko beam resting on elastic half-plane based on the coupling of locking-free finite elements and boundary integral", *Computational Mechanics*, vol. 45, no. 2-3, pp. 211-225, 2010, doi: 10.1007/s00466-009-0431-2.

[15] J. Li, Y. Zhu, S. Ye, and X. Ma, "Internal Force Analysis and Field Test of Lattice Beam Based on Winkler Theory for Elastic Foundation Beam", *Mathematical Problems in Engineering*, vol. 2019, art. no. 5130654, 2019, doi: 10.1155/2019/5130654.

[16] M. Ataman and W. Szcześniak, "Influence of Inertial Vlasov Foundation Parameters on the Dynamic Response of the Bernoulli–Euler Beam Subjected to A Group of Moving Forces – Analytical Approach", *Materials*, vol. 15, no. 9, art. no. 3249, 2022, doi: 10.3390/ma15093249.

[17] D. Froio, R. Moioli, and E. Rizzi, "Numerical dynamic analysis of beams on nonlinear elastic foundation under harmonic moving load", in *Proceedings of the VII European Congress on Computational Methods in Applied Sciences and Engineering (ECCOMAS Congress 2016)*. Crete Island, Greece: Institute of Structural Analysis and Antiseismic Research School of Civil Engineering National Technical University of Athens (NTUA) Greece, 2016, pp. 4794–4809, doi: 10.7712/100016.2149.7515.

[18] D. Zhu, E. Yan, and K. Song, "Research on interaction mechanism between lattice beam and slope rock mass and field test", *Chinese Journal of Rock Mechanics and Engineering*, vol. 28 no. S1, pp. 2947–2953, 2009, 10.13722/j.cnki.jrme.2023.0163.

[19] D. Han, Y. Men, and Z. Hu, "Experimental study of anti-sliding mechanism and force of lattice anchor in soil landslide", *Rock and Soil Mechanics*, vol. 41, no. 04, pp. 1189–1194+1202, 2020, doi: 10.16285/j.rsm.2019.0806.

[20] X. Lin, W. Liu, and Y. Que, "Stability Analysis and Treatment of High Fill Embankment Slope with Unfavorable Geology", *Highway Engineering*, vol. 48, no. 03, pp. 132–137, 2023, doi: 10.19782/j.cnki.1674-0610.2023.03.018.

[21] J. Tan, S. Fang, and X. Jiang, "Bearing capacity renewal of RC beams based on monitoring data and Bayesian theory", *Building Structure*, vol. 53, no. 16, pp. 91–97, 2023, doi: 10.19701/j.jzjg.20210107.

[22] N. Yu, et al., "Selection of a phase change material and its thickness for application in walls of buildings for solar-assisted steam curing of precast concrete", *Renewable Energy*, vol. 150, pp. 808–820, 2020, doi: 10.1016/j.renene.2019.12.130.

[23] Y. Huang and F. He, *Beams, slabs and shells on elastic foundations*. Beijing: Science Press, 2005.

[24] Y. Gai, H. Li, and L. Long, "Research on seismic performance of single tower asymmetric steel-mixed girder cable-stayed bridge", *Journal of Changsha University of Science & Technology (Natural Science)*, vol. 21, no. 04, pp. 149–159, 2024, doi: 10.19951/j.cnki.1672-9331.20231129001.

Received: 2024-09-22, Revised: 2024-12-06